PDMS-Coated S-Tapered Fiber for Highly Sensitive Measurements of Transverse Load and Temperature

Rui Yang, Yong-Sen Yu, Cong-Cong Zhu, Yang Xue, Chao Chen, Xuan-Yu Zhang, Bao-Lin Zhang, and Hong-Bo Sun, *Member, IEEE*

***Abstract*— A novel highly sensitive fiber sensor for transverse load and temperature measurement has been fabricated by polydimethylsiloxane (PDMS) packaging an S fiber taper (SFT). The PDMS coating is an effective transverse load and temperature transducer due to its material characteristics, such as low Young's modulus, high Poisson's ratio, and large thermooptic coefficient, which can efficiently transfer the lateral force into axial tension on the SFT or convert temperature into refractive index (RI) change around SFT. Because the SFT is highly sensitive to axial strain and surrounding RI, the PDMS-coated SFT will have high sensitivities of transverse load and temperature, which have been experimentally obtained up to −29.03 nm/N and −2.17 nm/°C, respectively. In addition, to solve the problem of cross sensitivity, two-wavelength demodulation method has been proposed for simultaneous measurement of transverse load and temperature.**

***Index Terms*— Fiber optic sensors, polydimethylsiloxane (PDMS), fiber taper, transverse load sensors, temperature sensors.**

I. Introduction

FOR decades, optical fiber sensors have found increasing applications in physical and chemical sensing fields due to their salient merits of high sensitivity, small size, fast response, corrosion resistance and so on. Up to now, various types of fiber sensors have been proposed and demonstrated, such as fiber Bragg gratings (FBGs) [1], [2], long period fiber gratings (LPFGs) [3], [4], fiber Mach-Zehnder interferometers (FMZIs) [5]–[7], fiber loop mirrors (FLMs) [8], [9], and other structures [10]–[12]. They have been extensively used for measurements of temperature [13]–[15], strain [5], [6], refractive index [3], [4], [7], transverse load [16]–[29], etc. In terms of transverse load sensing, different FBGs inscribed in single-mode fiber (SMF) [16], highly-birefringent fiber [17], and microstructured fiber [18], [19] have been reported. These FBGs exhibited a pronounced polarization mode split effect resulting from the birefringence induced by the transverse load. The splitting and shifting of the Bragg reflection peaks of two orthogonal polarization modes can be used to measure the magnitude and orientation of the transverse load. To further improve the transverse load sensitivity, FBGs have been packaged by polymer coating, which has low stiffness and will efficiently transfer the force applied in the radial direction to the perpendicular plane, enhancing the transverse load sensitivity to 0.3 nm/(N/mm) [20]. Besides, the LPFG, as a promising fiber sensor, also has been demonstrated to measure the transverse load by using the load induced birefringence in the fiber [21]. Its transverse load sensitivity reaches as high as 50 nm/(N/mm). However, these kinds of fiber grating-based (FBGs and LPFGs) transverse load sensors usually need high cost and complicated fabrication technology, including laser source and precise optical path. In addition, complex detection systems are required to monitor the polarization mode splitting effect. In order to simplify the fabrication and detection process, some new fiber sensor structures for transverse load measurement have been proposed in recent years. A simple structured FMZI based on two fiber tapers has been reported as a transverse load sensor, which can also detect the loading position information along the fiber interferometer [22]. Another fiber transverse load sensor is formed by using a short section of photonic crystal fiber (PCF) which is inserted inside a Sagnac fiber loop [8]. An initial transverse force is required to apply on the PCF to introduce necessary birefringence for measurement. Moreover, a low cost fiber-tip micro-cavity, worked as a Fabry-Perot interferometer, is fabricated for measurement of transverse load and achieves a high sensitivity of 1.37 nm/N [23]. This sensor will be used for temperature sensing as well. Its temperature sensitivity is about 2.1 pm/°C. In order to develop more sensitive fiber sensors, new structures should be further explored.

In this paper, we demonstrate a new fiber sensor based on polydimethylsiloxane (PDMS)-coated S fiber taper (SFT) for highly sensitive measurements of transverse load and temperature. The SFT is fabricated by tapering the SMF with a certain axial offset in a fusion splicer [7]. Then, it is packaged in a cuboid PDMS coating with a length of 10 mm. Because the PDMS material has low elastic modulus and high Poisson's ratio coefficient, external transverse force on the PDMS coating will be efficiently converted into the axial tension on

Manuscript received October 22, 2014; revised December 12, 2014; accepted December 21, 2014. Date of publication January 7, 2015; date of current version April 22, 2015. This work was supported by the National Basic Research Program of China (973 Program) under Grant 2011CB013003 and Grant 2014CB921302, and by the National Natural Science Foundation of China under Grant 61435005, Grant 91323301, and Grant 91423102. The work of H.-B. Sun was supported by the Program for Changjiang Scholars and Innovative Research Team at University, China, in 2007. The associate editor coordinating the review of this paper and approving it for publication was Dr. Anupama Kaul.

The authors are with the State Key Laboratory on Integrated Optoelectronics, College of Electronic Science and Engineering, Jilin University, Changchun 130012, China (e-mail: yuys@jlu.edu.cn; hbsun@jlu.edu.cn).

Color versions of one or more of the figures in this paper are available online at http://ieeexplore.ieee.org.

Digital Object Identifier 10.1109/JSEN.2015.2388490

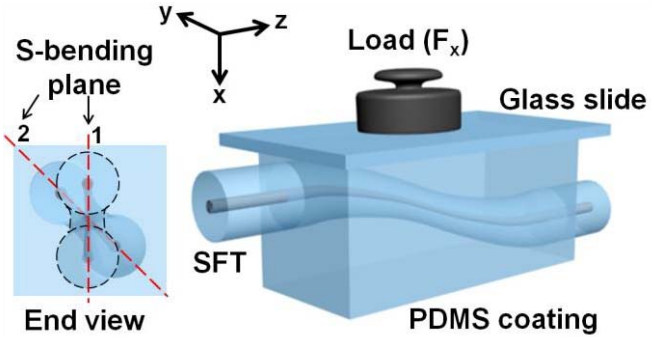

Fig. 1. Schematic diagram of PDMS-coated SFT and the experimental setup for transverse load sensing. The S-bending planes 1 and 2 are parallel to x-axis and 45° angle to the x-axis, respectively.

the SFT. According to our previous work [30], the SFT is highly sensitive to axial strain, so this sensor will realize a high sensitivity for transverse load measurement. In addition, the PDMS also has large thermo-optic coefficient (TOC) and thermal expansion coefficient (TEC). With temperature increase, the refractive index (RI) of PDMS will decrease and the size of the PDMS coating along the fiber will expand. Both the change will make the transmission spectrum of the SFT moving to short wavelength. These thermo-optic effect and thermal expansion effect overlap each other and make the sensor highly sensitive to temperature. We theoretically analyze the transverse load and temperature sensing mechanisms for the sensor, and carry out the corresponding experiments. When the SFT is positioned with S-bending plane parallel to x-axis, as shown in Fig. 1 (S-bending plane 1), the maximum load sensitivity reaches −29.03 nm/N, which is 21 times higher than that of the fiber-tip micro-cavity sensor [23]. When the S-bending plane 2 is chosen, the results show that the maximum load sensitivity is −8.05 nm/N, and the temperature sensitivity achieves −2.17 nm/°C.

II. Fabrication

The schematic diagrams of the PDMS-coated SFT and the transverse load sensing experimental setup are shown in Fig. 1. The SFT is positioned at the center of the PDMS block. In the end view, the S-bending plane can be positioned parallel to the x-axis or 45° angle to the side face of the cuboid PDMS coating, corresponding to the S-bending planes 1 and 2, respectively. If the S-bending plane 1 is chosen, the sensor will have different load sensitivities when the transverse force direction is along with the x-axis or y-axis due to the asymmetric structure of the SFT. In the case of S-bending plane 2, the sensor will have the same load response regardless of the transverse force direction.

The SFT was fabricated on the standard telecom SMF (SMF-28e, Corning, Inc.) by a fusion splicer (Ericsson FSU-975). It operated as a fiber Mach-Zehnder interferometer and the detailed fabrication process was reported in ref. [30]. During the fabrication process, a supercontinuum broadband source (Superk Compact, NKT Photonics, Inc.) provided the input light and an optical spectrum analyzer (OSA) (Yokogawa AQ6370B) was used to monitor

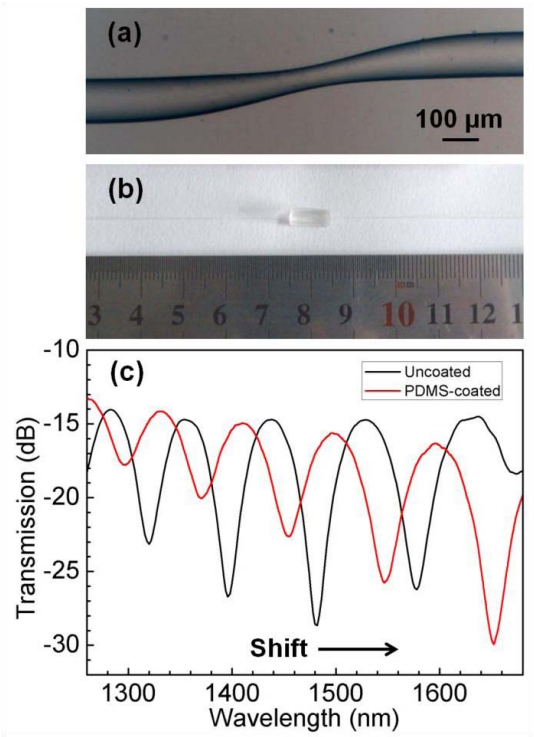

Fig. 2. (a) Optical microscope image of the SFT. (b) Image of the PDMS-coated SFT with the size of 3 mm × 3 mm × 10 mm. (c) Transmission spectrum of the SFT before and after PDMS coating.

and record the transmission spectrum of the SFT. In the experiment, we set the discharge current, tapering time and fiber holders' axial offset to 10 mA, 10 s and 160 μm, respectively. The obtained SFT is shown in Fig. 2(a), which has the structure parameters of about 820 μm in length, 64 μm in waist diameter, and 125 μm in axial offset, respectively. Then the SFT was put into a Teflon mold with a cuboid groove (3 mm × 3 mm × 10 mm). The position of the SFT was carefully adjusted under an optical microscope. Here, we fabricated the sensor with S-bending plane 2, namely the S-bending plane has 45° angle to the side face of the cuboid groove. Furthermore, according to our previous work [30], the SFT has a two-fold linear response to axial strain. When an initial axial tension adds to the SFT, the S-shape may have a rapid change, resulting in larger axial strain sensitivity. In order to get one-fold linear behavior, we applied a prestress of about 0.2 N on the SFT when it was packaged. The black curve in Fig. 2(c) (uncoated) is the transmission spectrum of the SFT under axial tension. Later, the PDMS solution with a 10:1 mixing ratio of precursor of elastic material and hardener was decanted into the Teflon mold. The mold was then put in a thermostat at 100 °C. The prepolymer of the mixture was polymerized by baking it in the thermostat for 2 hours. Finally, the PDMS-coated SFT sensor was obtained after removing the mold. As shown in Fig. 2(b), the sensor has the structure size of 3 mm × 3 mm × 10 mm. In Fig. 2(c), the transmission spectra between uncoated (RI = 1.00) SFT and PDMS-coated (RI = 1.40) sensor are different due to the phase matching conditions of the interference are changed by surrounding RI. According to the

reported work [30], the transmission spectrum of the SFT has a red shift with the increase of surrounding RI. So the PDMS-coated sensor has a transmission spectrum moving to longer wavelength compared with the uncoated SFT.

Since the SFT is just hundreds of microns in length, the PDMS-coated sensor size could be further shortened to about 1 mm. With such a small size, the sensor will be used in small areas such as blood vessels.

III. Sensing Mechanisms

The fabricated sensor integrates the characteristics of the SFT and PDMS material, making it highly sensitive to transverse load and temperature. As reported in [30], the SFT has high sensitivities for RI and axial strain measurement but insensitive to temperature. The PDMS material has low Young's modulus ($E_P = 750\ kPa$) and high Poisson's ratio coefficient ($\eta = 0.45$). When the SFT is packaged by the PDMS block, which can be a transducer and efficiently convert the transverse stress on the PDMS coating into the axial tension on the SFT, a highly sensitive transverse load sensor will be realized. Moreover, the PDMS also has high TEC ($\alpha_P^T = 300\ \mu\varepsilon/°\text{C}$) and TOC ($\gamma_P^{TO} = -1.5 \times 10^{-4} \sim -5.0 \times 10^{-4}\ /°\text{C}$) [31]. With temperature augment, the thermal expansion effect of the PDMS will increase the axial strain on the SFT and the thermo-optic effect of the PDMS will decrease the RI around the SFT. Both the changes results in the transmission spectrum of the SFT moving to short wavelength. So the PDMS coating is also a temperature transducer and makes the sensor highly sensitive to temperature. The sensing mechanisms of the sensor for transverse load and temperature measurement will be simply analyzed below.

A. Transverse Load Sensing Mechanism

In Fig. 1, when transverse load (F_x) is added on the PDMS block along the x-axis direction, the PDMS will expand in y- and z-axis directions. If the SFT is not in the PDMS, according to the Hooke's law, strain in the PDMS along z-axis is

$$\varepsilon_P = \eta \frac{F_x}{A_P^{yz} E_P}, \tag{1}$$

where A_P^{yz} is the compression area on the PDMS. When the SFT is embedded in the PDMS coating, reciprocal force (F_r) between them will occur under transverse load and decrease the PDMS strain ε_P. Considering the SFT and PDMS having the same total axial strain (ε), which can be written as

$$\varepsilon = \varepsilon_f^r = \varepsilon_P - \varepsilon_P^r, \tag{2}$$

where ε_f^r is the axial strain of SFT under F_r and ε_P^r is the axial strain decrement of the PDMS under F_r. Here, the reciprocal force is expressed as

$$F_r = A_f E_f \varepsilon_f^r = A_P^{xy} E_P \varepsilon_P^r, \tag{3}$$

where A_f and E_f (72 GPa) are the sectional area and Young's modulus of the optical fiber, respectively, A_P^{xy} is the cross-sectional area of the PDMS coating along z-axis. Based on the equations (1) to (3), the relationship between axial strain of the SFT (ε_f^z) and transverse load on the sensor can be deduced as

$$\varepsilon_f^z = \varepsilon_f^r = \eta \frac{A_P^{xy}}{A_P^{yz}(A_P^{xy} E_P + A_f E_f)} F_x. \tag{4}$$

So the axial strain on SFT per unit transverse load is

$$k_F = \frac{\varepsilon_f^z}{F_x} = \eta \frac{A_P^{xy}}{A_P^{yz}(A_P^{xy} E_P + A_f E_f)}. \tag{5}$$

Substituting the values of each parameter into expression (5), we get $k_F = 151.7\ \mu\varepsilon/N$. In our previous work [30], the SFT has the average axial strain sensitivity ranging from $-80\ \text{pm}/\mu\varepsilon$ to $-180\ \text{pm}/\mu\varepsilon$. However, when the axial tension on SFT is above 2.0 N, the strain sensitivity decreases to below the average values. For the sensor in our experiment, because the embedded SFT has a prestress of 2.0 N, its axial strain sensitivity could be assumed to a small value of $-50\ \text{pm}/\mu\varepsilon$. So the transverse load sensitivity of the sensor is simply estimated to -7.585 nm/N. It should be noted that the shape of SFT will also change under transverse load, further increasing the sensitivity.

B. Temperature Sensing Mechanism

Actually, there are three aspects to contribute to the temperature sensitivity, including the thermal expansion and thermo-optic effects of the PDMS coating and shape change of the SFT. So the total temperature sensitivity (S_T) of the sensor can be written as

$$S_T = S_T^{TE} + S_T^{TO} + S_T^{SC}, \tag{6}$$

where S_T^{TE} and S_T^{TO} are the temperature sensitivity contributions (TSC) from thermal expansion and thermo-optic effects of PDMS, respectively, S_T^{SC} is the TSC from shape change of SFT in PDMS when temperature changes.

Although the PDMS has a high TEC, its Young's modulus is too low, leading to a small S_T^{TE}. Its value is computed as follows.

With temperature increase (ΔT), optical fiber (ε_f^T) and PDMS (ε_P^T) will expand and axial strain in them can be expressed as

$$\varepsilon_f^T = \alpha_f^T \Delta T, \tag{7}$$

$$\varepsilon_P^T = \alpha_P^T \Delta T, \tag{8}$$

where α_f^T and α_P^T are the TECs of fiber and PDMS, respectively. Because the two TECs are different, reciprocal force (F_r) between the SFT and PDMS will occur with temperature augment, resulting in a strain increment (ε_f^r) on SFT and strain decrement (ε_P^r) on PDMS along z-axis. The total strain change (ε) on SFT and PDMS are the same and written as

$$\varepsilon = \varepsilon_f^T + \varepsilon_f^r = \varepsilon_P^T - \varepsilon_P^r. \tag{9}$$

The reciprocal force between SFT and PDMS coating has the same form with equation (3). According to the equations

above, the axial strain change on SFT with temperature can be deduced as

$$\varepsilon_f^z = \varepsilon_f^T + \varepsilon_f^r = \left[\alpha_f^T + (\alpha_P^T - \alpha_f^T)\frac{A_P^{xy} E_P}{A_P^{xy} E_P + A_f E_f}\right]\Delta T. \tag{10}$$

So the axial strain change on SFT per unit temperature is

$$k_T = \frac{\varepsilon_f^z}{\Delta T} = \alpha_f^T + (\alpha_P^T - \alpha_f^T)\frac{A_P^{xy} E_P}{A_P^{xy} E_P + A_f E_f}. \tag{11}$$

Substituting the values of each parameter into expression (11), we obtain $k_T = 2.82\ \mu\varepsilon/°\text{C}$. Since the axial strain sensitivity of the SFT is assumed to $-50\ \text{pm}/\mu\varepsilon$, the TSC from thermal expansion effect of PDMS is $S_T^{TE} = -141\ pm/°\text{C}$.

In addition, the TSC from thermo-optic effect of PDMS can be expressed as

$$S_T^{TO} = \gamma_P^{TO} S_{RI}, \tag{12}$$

where S_{RI} is RI sensitivity of the SFT. In our experiment, it has achieved 2000 nm/RI unit (RIU) when the ambient RI is around 1.40 (RI of PDMS coating). The TOC (γ_P^{TO}) of PDMS has a high value up to -5.0×10^{-4} /°C. If we choose this value, thermo-optic effect of the PDMS coating contributes a temperature sensitivity (S_T^{TO}) of -1.0 nm/°C, which is much larger than that of S_T^{TE}.

When temperature change, the volume of PDMS coating will expand or shrink, leading to shape change of the embedded SFT. Because of transmission spectrum of the SFT also sensitive to its geometrical structure, this will contribute to the temperature sensitivity as well.

IV. Sensing Characteristics

A. Transverse Load Sensing

The sensor was used for transverse load measurement by using the experimental setup in Fig. (1). A piece of glass slide was put on the top face y-z of the sensor to get uniform transverse stress. Then a set of weights were added onto the glass slide one by one. At each step, transmission spectrum of the sensor was recorded by the OSA. The experimental results are shown in Fig. 3(a). With transverse load increase, the transmission spectrum of the sensor moves to short wavelength and the attenuation dips are weakened. That's because the PDMS coating will convert the transverse load into axial strain on the SFT. Its transmission spectrum has a blueshift with the axial strain increase [30]. Meanwhile, the S bending shape is straightened. Less light energy will be coupled from core mode into cladding modes or reverse, leading to the light interference weakened quickly. Later, the sensor was rotated 90° along z-axis and the transverse load experiment was repeated on side face x-z to examine the sensor's consistency in different transverse force direction. We marked three resonant dips in the transmission spectrum and plotted their wavelength change with different load, as shown in Fig. 3(b). Load tests 1 and 2 are the experimental results when transverse load direction on two perpendicular side-face of the sensor. Their slopes have some error due to the position of the S-bending plane not exactly 45° to the side face of the PDMS coating. In load test 1, the linear fitting results, namely the transverse load sensitivities, for the resonant dips A, B and C are -7.23 nm/N, -6.69 nm/N, and -6.04 nm/N, respectively. In load test 2, the corresponding sensitivities are -8.05 nm/N, -8.01 nm/N, and -7.15 nm/N, respectively. The errors in these two cases could be further minished by more precise adjustment. Anyhow, this sensor presents a high sensitivity for transverse load measurement.

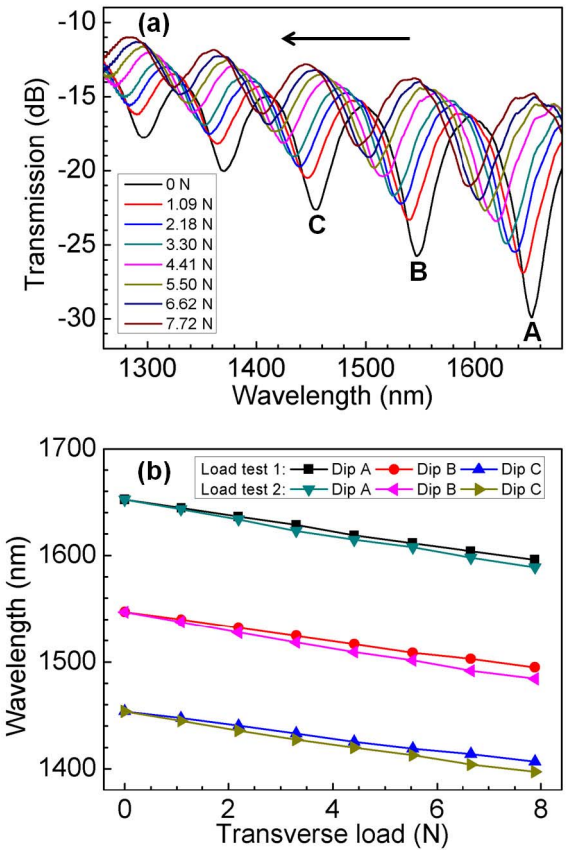

Fig. 3. (a) Transmission spectrum of the sensor with S-bending plane 2 changes under different transverse load. (b) Relationships between transverse load and wavelength of the resonant dips A, B and C. Load tests 1 and 2 represent the transverse load directions in x-axis and y-axis, respectively, in Fig. 1.

In addition, we fabricated another SFT with geometrical parameters of 851 μm in length, 64 μm in waist diameter, and 140 μm in axial offset, respectively, and packaged it with the S-bending plane 1 position for comparison. There is no prestress when the SFT was packaged, so the sensor will have two-fold linear response to transverse load. We carried out the transverse load experiment and the results are shown in Fig. 4. Load tests 1 and 2 mean the transverse force direction in x-axis and y-axis, respectively. They have very different transverse load response owing to the asymmetric structure of the SFT. When the transverse load direction is in x-axis, the shape of the SFT will have much larger change than that of y-axis case, resulting in a higher sensitivity. Moreover, for each load test, the results have two-fold linear response ranges. When the transverse load is below 2.18 N, the linear fitting results, namely the transverse load sensitivities are

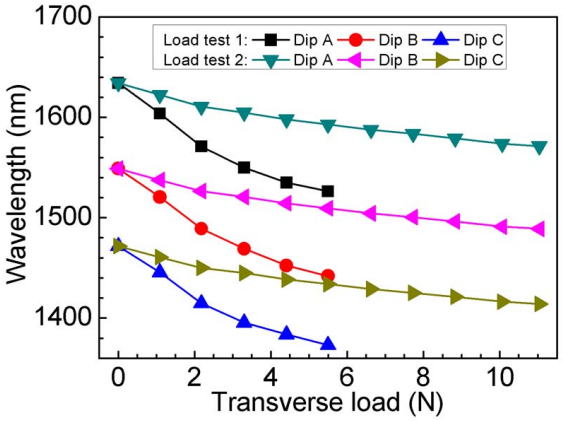

Fig. 4. Transverse load experimental results for the sensor with S-bending plane 1. The plots are relationships between transverse load and wavelength of the resonant dips A, B and C, respectively.

higher than that of transverse load above 2.18 N. In load test 1, when the transverse load ranges from 0 to 2.18 N, the sensitivities for the three resonant dips are −29.03 nm/N, −27.46 nm/N, and −26.18 nm/N, respectively. When the load changes from 2.18 N to 5.50 N, the sensitivities are −13.50 nm/N, −14.33 nm/N, and −12.32 nm/N. In load test 2, when the transverse load is below 2.18 N, the sensitivities for the resonant dips are −10.80 nm/N, −10.33 nm/N, and −9.96 nm/N, respectively. When the load continued to increase from 2.18 N to 11.04 N, the sensitivities are −4.46 nm/N, −4.26 nm/N, and −4.09 nm/N, respectively. In this case of S-bending plane 1, the sensor can realize a high sensitivity up to −29.03 nm/N, which is 21 times higher than that of the fiber-tip micro-cavity sensor. Under this sensitivity, the detection limit could reach 6.89×10^{-4} N with the OSA resolution of 0.02 nm.

However, the nonlinear behavior of the sensor is not good for demodulation in practical applications. So we still use the sensor with S-bending plane 2 for temperature experiment.

B. Temperature Sensing

To test temperature response, the sensor was immersed into an oil bath, which has a temperature resolution of 0.01 °C. The oil bath was heated up from 20 °C to 65 °C in steps of 2.5 °C. At each step, the temperature was kept for 10 minutes and the transmission spectrum of the sensor was recorded after it stabled. With temperature increase, the transmission spectrum moves to short wavelength, as shown in Fig. 5(a). The extinction ratio (ER) of resonant dips A, B and C are increasing. This phenomenon is different from that in transverse load test, which has a decreased ER. Because in temperature sensing, the axial strain change on SFT by thermal expansion effect of PDMS has less impact on the transmission spectrum compared with the RI change around SFT by thermo-optic effect of PDMS. The wavelength changes with temperature for the three resonant dips are plotted in Fig. 5(b). They have good linear response and the fitting results, namely temperature sensitivities, are −2.17 nm/°C, −1.99 nm/°C, and −1.83 nm/°C, respectively. According to the analysis of temperature sensing mechanism, the TSCs from thermal

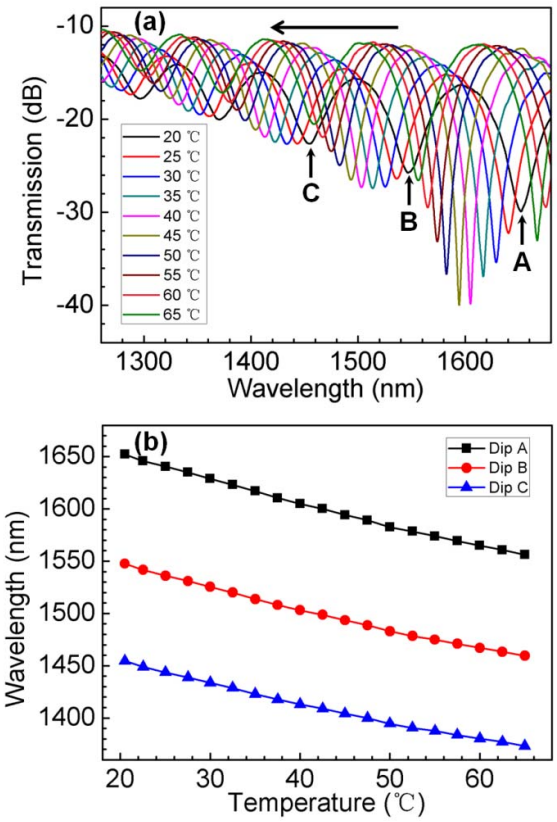

Fig. 5. (a) Transmission spectrum of the sensor changes at different temperature. (b) Relationships between temperature and wavelength of the resonant dips A, B and C, respectively.

expansion effect and thermo-optic effect are −0.14 nm/°C and −1.00 nm/°C, respectively. Their sum (−1.14 nm/°C) is still much less than the experimental results. This means the shape change of the SFT also affords a large TSC to the sensor. The temperature sensitivity of this sensor is much higher than most liquid-sealed FMZI sensors [15], [32], [33] and more robust. It will be a promising fiber temperature sensor for highly sensitive biological sensing.

C. Simultaneous Measurement of Transverse Load and Temperature

Because of the PDMS-coated S-tapered fiber simultaneous highly sensitive to transverse load and temperature, this will lead to a problem of temperature cross-sensitivity while measurement of transverse load. Fortunately, the transmission spectrum has multi-resonant dips with different response to transverse load and temperature. We can monitor the wavelength change of two dips and establish a sensitivity matrix to solve the variations of transverse load and temperature simultaneously. If we choose resonant dips A and B, the wavelength change ($\Delta\lambda_A$, $\Delta\lambda_B$) as functions of transverse load and temperature (ΔF, ΔT) can be expressed as

$$\begin{bmatrix} \Delta\lambda_A \\ \Delta\lambda_B \end{bmatrix} = \begin{bmatrix} K_A^F & K_A^T \\ K_B^F & K_B^T \end{bmatrix} \begin{bmatrix} \Delta F \\ \Delta T \end{bmatrix}, \tag{13}$$

where K_A^F and K_B^F are the transverse load sensitivities of the dips A and B, respectively, K_A^T and K_B^T are their temperature

sensitivities. In the experiment, for the sensor with S-bending plane 2, if the transverse load is in x-axis, we get the sensitivity matrix as $\begin{bmatrix} -7.23 & -2.17 \\ -6.69 & -1.99 \end{bmatrix}$. This two-wavelength demodulation method will be an effective way to solve the problem of cross-sensitivity in practical applications.

Moreover, if the sensor with S-bending plane 1 is used for simultaneous measurements, the nonlinear spectral response should be divided into two-fold linear responses and two sensitivity matrix are required, which will complicate the demodulating process.

In practical applications, it's important to demodulate external changes with different directions. The transverse force direction could be predicted by two sensors with S-bending plane 1 in parallel. One of the sensors has an S-bending plane perpendicular to the other sensor. With this combination structure, the sensor with the S-bending plane parallel to the transverse direction will has a larger wavelength change. By the sensor, the highly sensitive transverse load measurements could also be realized. However, this direction predictable solution makes the sensor structure more complex.

In addition, for a broader use of the sensor in the fields where environment moisture and solvent composition is important and the polymer swelling issue should be considered. The polymer swelling can significantly change performance of opto-fluidic devices [34]. For the PDMS-coated sensor, due to the SFT very sensitive to the properties of PDMS, the sensing characteristics of the device will change with the PDMS swelling in high humidity atmosphere or other environment. To solve the problem, the sensor should be further encapsulated to avoid influences of environment moisture and solvents.

V. Conclusion

In conclusion, we have demonstrated a highly sensitive fiber sensor for transverse load and temperature measurement. This sensor is fabricated by PDMS packaging an SFT, which is formed through off-axis stretched SMF in a fusion splicer. We have simply analyzed the working principle for the sensor and deduced its sensing expressions. Thanks to the PDMS features, including low Young's modulus, high Poisson's ratio coefficient, and large thermo-optic coefficient, the sensor has extremely high sensitivities of transverse load and temperature, which are experimentally obtained up to -29.03 nm/N and -2.17 nm/°C, respectively. Moreover, the two-wavelength demodulation method has been proposed to simultaneous measurement of transverse load and temperature. This sensor is simple structured, cost effectiveness and easy of fabrication. It will find applications in physical and biological sensing fields.

References

[1] P. S. Reddy *et al.*, "Method for enhancing and controlling temperature sensitivity of fiber Bragg grating sensor based on two bimetallic strips," *IEEE Photon. J.*, vol. 4, no. 3, pp. 1035–1041, Jun. 2012.

[2] C. Chen *et al.*, "Monitoring thermal effect in femtosecond laser interaction with glass by fiber Bragg grating," *J. Lightw. Technol.*, vol. 29, no. 14, pp. 2126–2130, Jul. 15, 2011.

[3] X. Shu, L. Zhang, and I. Bennion, "Sensitivity characteristics of long-period fiber gratings," *J. Lightw. Technol.*, vol. 20, no. 2, pp. 255–266, Feb. 2002.

[4] J.-C. Guo *et al.*, "Compact long-period fiber gratings with resonance at second-order diffraction," *IEEE Photon. Technol. Lett.*, vol. 24, no. 16, pp. 1393–1395, Aug. 15, 2012.

[5] P. Lu and Q. Chen, "Asymmetrical fiber Mach–Zehnder interferometer for simultaneous measurement of axial strain and temperature," *IEEE Photon. J.*, vol. 2, no. 6, pp. 942–953, Dec. 2010.

[6] D. Wu, T. Zhu, K. S. Chiang, and M. Deng, "All single-mode fiber Mach–Zehnder interferometer based on two peanut-shape structures," *J. Lightw. Technol.*, vol. 30, no. 5, pp. 805–810, Mar. 1, 2012.

[7] R. Yang, Y. S. Yu, Y. Xue, C. Chen, Q.-D. Chen, and H.-B. Sun, "Single S-tapered fiber Mach–Zehnder interferometers," *Opt. Lett.*, vol. 36, no. 23, pp. 4482–4484, Dec. 2011.

[8] P. Zu, C. C. Chan, Y. Jin, Y. Zhang, and X. Dong, "Fabrication of a temperature-insensitive transverse mechanical load sensor by using a photonic crystal fiber-based Sagnac loop," *Meas. Sci. Technol.*, vol. 22, no. 2, pp. 025204-1–025204-4, Jan. 2011.

[9] W. Qian *et al.*, "High-sensitivity temperature sensor based on an alcohol-filled photonic crystal fiber loop mirror," *Opt. Lett.*, vol. 36, no. 9, pp. 1548–1550, May 2012.

[10] A. M. Hatta, Y. Semenova, Q. Wu, and G. Farrell, "Strain sensor based on a pair of single-mode–multimode–single-mode fiber structures in a ratiometric power measurement scheme," *Appl. Opt.*, vol. 49, no. 3, pp. 536–541, Jan. 2010.

[11] Y. Xue *et al.*, "Ultrasensitive temperature sensor based on an isopropanol-sealed optical microfiber taper," *Opt. Lett.*, vol. 38, no. 8, pp. 1209–1211, Apr. 2013.

[12] X.-Y. Zhang *et al.*, "Miniature end-capped fiber sensor for refractive index and temperature measurement," *IEEE Photon. Technol. Lett.*, vol. 26, no. 1, pp. 7–10, Jan. 1, 2014.

[13] Y. Geng, X. Li, X. Tan, Y. Deng, and Y. Yu, "High-sensitivity Mach–Zehnder interferometric temperature fiber sensor based on a waist-enlarged fusion bitaper," *IEEE Sensors J.*, vol. 11, no. 11, pp. 2891–2894, Nov. 2011.

[14] C.-S. Park, K.-I. Joo, S.-W. Kang, and H.-R. Kim, "A PDMS-coated optical fiber Bragg grating sensor for enhancing temperature sensitivity," *J. Opt. Soc. Korea*, vol. 15, no. 4, pp. 329–334, Dec. 2011.

[15] S. J. Qiu, Y. Chen, F. Xu, and Y.-Q. Lu, "Temperature sensor based on an isopropanol-sealed photonic crystal fiber in-line interferometer with enhanced refractive index sensitivity," *Opt. Lett.*, vol. 37, no. 5, pp. 863–865, Mar. 2012.

[16] A.-P. Zhang, B.-O. Guan, X.-M. Tao, and H.-Y. Tam, "Experimental and theoretical analysis of fiber Bragg gratings under lateral compression," *Opt. Commun.*, vol. 206, nos. 1–3, pp. 81–87, May 2002.

[17] H.-M. Kim, T.-H. Kim, B. Kim, and Y. Chung, "Enhanced transverse load sensitivity by using a highly birefringent photonic crystal fiber with larger air holes on one axis," *Appl. Opt.*, vol. 49, no. 20, pp. 3841–3845, Jul. 2010.

[18] C. Jewart *et al.*, "Sensitivity enhancement of fiber Bragg gratings to transverse stress by using microstructural fibers," *Opt. Lett.*, vol. 31, no. 15, pp. 2260–2262, Aug. 2006.

[19] T. Geernaert *et al.*, "Transversal load sensing with fiber Bragg gratings in microstructured optical fibers," *IEEE Photon. Technol. Lett.*, vol. 21, no. 1, pp. 6–8, Jan. 1, 2009.

[20] B. K. A. Ngoi, J. Paul, L. P. Zhao, and Z. P. Fang, "Enhanced lateral pressure tuning of fiber Bragg gratings by polymer packaging," *Opt. Commun.*, vol. 242, nos. 4–6, pp. 425–430, Dec. 2004.

[21] Y. Liu, L. Zhang, and I. Bennion, "Fibre optic load sensors with high transverse strain sensitivity based on long-period gratings in B/Ge co-doped fibre," *Electron. Lett.*, vol. 35, no. 8, pp. 661–663, Apr. 1999.

[22] P. Lu, G. Lin, X. Wang, L. Chen, and X. Bao, "Lateral stress detection using a tapered fiber Mach–Zehnder interferometer," *IEEE Photon. Technol. Lett.*, vol. 24, no. 22, pp. 2038–2041, Nov. 15, 2012.

[23] J. Ma, J. Ju, L. Jin, W. Jin, and D. Wang, "Fiber-tip micro-cavity for temperature and transverse load sensing," *Opt. Exp.*, vol. 19, no. 13, pp. 12418–12426, Jun. 2011.

[24] C. M. Jewart *et al.*, "Suspended-core fiber Bragg grating sensor for directional-dependent transverse stress monitoring," *Opt. Lett.*, vol. 36, no. 12, pp. 2360–2362, Jun. 2011.

[25] J. Limpert *et al.*, "Yb-doped large-pitch fibres: Effective single-mode operation based on higher-order mode delocalisation," *Light Sci. Appl.*, vol. 1, p. e8, Apr. 2012.

[26] M. Silva-Lopez *et al.*, "Differential birefringence in Bragg gratings IN multicore fiber under transverse stress," *Opt. Lett.*, vol. 29, no. 19, pp. 2225–2227, Oct. 2004.

[27] C. Chen *et al.*, "Compact fiber tip modal interferometer for high-temperature and transverse load measurements," *Opt. Lett.*, vol. 38, no. 17, pp. 3202–3204, Sep. 2013.
[28] Y.-L. Sun *et al.*, "Protein-based soft micro-optics fabricated by femtosecond laser direct writing," *Light Sci. Appl.*, vol. 3, p. e129, Jan. 2014.
[29] G. T. Kanellos, G. Papaioannou, D. Tsiokos, C. Mitrogiannis, G. Nianios, and N. Pleros, "Two dimensional polymer-embedded quasi-distributed FBG pressure sensor for biomedical applications," *Opt. Exp.*, vol. 18, no. 1, pp. 179–186, Jan. 2010.
[30] R. Yang *et al.*, "S-tapered fiber sensors for highly sensitive measurement of refractive index and axial strain," *J. Lightw. Technol.*, vol. 30, no. 19, pp. 3126–3132, Oct. 1, 2012.
[31] J. Barnes, M. Dreher, K. Plett, R. S. Brown, C. M. Crudden, and H. P. Loock, "Chemical sensor based on a long-period fibre grating modified by a functionalized polydimethylsiloxane coating," *Analyst*, vol. 133, no. 11, pp. 1541–1549, Nov. 2008.
[32] W. Qian *et al.*, "Temperature sensing based on ethanol-filled photonic crystal fiber modal interferometer," *IEEE Sensors J.*, vol. 12, no. 8, pp. 2593–2597, Aug. 2012.
[33] R. Yang *et al.*, "A highly sensitive temperature sensor based on a liquid-sealed S-tapered fiber," *IEEE Photon. Technol. Lett.*, vol. 25, no. 9, pp. 829–832, May 1, 2013.
[34] G. Gervinskas, D. Day, and S. Juodkazis, "High-precision interferometric monitoring of polymer swelling using a simple optofluidic sensor," *Sens. Actuators B, Chem.*, vol. 159, no. 1, pp. 39–43, Jun. 2011.

Rui Yang received the B.S. degree in microelectronics from the College of Electronic Science and Engineering, Jilin University, Changchun, China, in 2009, where he is currently pursuing the Ph.D. degree. His current research interests include femtosecond laser fabrication of fiber gratings and fiber optic sensors.

Yong-Sen Yu received the M.S. degree in electronics from the Changchun University of Science and Technology, Changchun, China, in 2000, and the Ph.D. degree from the College of Electronic Science and Engineering, Jilin University, Changchun, in 2005.

He was an Associate Professor with the State Key Laboratory of Integrated Optoelectronics, Jilin University, in 2009. His current research interests include laser microfabrication, fiber gratings, and fiber optic sensors.

Cong-Cong Zhu received the B.S. degree in electronics science and technology from the College of Electronic Science and Engineering, Jilin University, Changchun, China, in 2012, where she is currently pursuing the M.S. degree. Her current research interests include femtosecond laser fabrication of fiber gratings and fiber optic sensors.

Yang Xue received the B.S. degree in electronics science and technology from the College of Electronic Science and Engineering, Jilin University, Changchun, China, in 2011, where he is currently pursuing the M.S. degree. His current research interests include femtosecond laser fabrication of fiber gratings and fiber optic sensors.

Chao Chen received the B.S. and M.S. degrees in electronics science and technology from the College of Electronic Science and Engineering, Jilin University, Changchun, China, in 2005 and 2010, respectively, where he is currently pursuing the Ph.D. degree. His current research interests include femtosecond laser fabrication of fiber gratings and fiber optic sensors.

He was an Engineer with Ibiden Electronics Beijing Company Ltd., Beijing, China, from 2005 to 2007.

Xuan-Yu Zhang received the B.S. degree in microelectronics from the College of Electronic Science and Engineering, Jilin University, Changchun, China, in 2012, where he is currently pursuing the M.S. degree. His current research interests include femtosecond laser fabrication of fiber gratings and fiber optic sensors.

Bao-Lin Zhang received the B.S. and M.S. degrees in semiconductor physics and devices physics from the Department of Electronic Science, Jilin University, Changchun, China, in 1986 and 1989, respectively, and the Ph.D. degree in condensed matter physics from the Institute of Physics, Chinese Academy of Sciences, Changchun, in 1999.

He was a Post-Doctoral Researcher with the Department of Physics, University of Oxford, Oxford, U.K., from 1999 to 2000, and a Researcher with Nanyang Technological University, Singapore, from 2001 to 2003. He has been in charge of the MOCVD Laboratory with the State Key Laboratory on Integrated Optoelectronics, Jilin University, since 2004, where he is currently a Full Professor. His current research interests include wide bandgap semiconductors (GaN and ZnO) and mid-infrared antimonide materials. He has authored over 70 scientific papers.

Hong-Bo Sun received the B.S. and Ph.D. degrees in electronics from Jilin University, Changchun, China, in 1992 and 1996, respectively.

He was a Post-Doctoral Researcher with the Satellite Venture Business Laboratory, University of Tokushima, Tokushima, Japan, from 1996 to 2000, and an Assistant Professor with the Department of Applied Physics, Osaka University, Osaka, Japan. In 2005, he was promoted to Full Professor (Changjiang Scholar) with Jilin University. His research has focused on laser micronanofabrication in the past ten years, in particular, in exploring novel laser technologies, including direct writing and holographic lithography, and their applications on microoptics, micromachines, microfluids, and microsensors. He has authored over 60 scientific papers in the above field, which have been cited for more than 3000 times according to ISI search report.

Prof. Sun became a Project Leader under the Precursory Research for Embryonic Science and Technology program in Japan in 2001, and received the National Natural Science Funds for Distinguished Young Scholar, China, in 2005. He was awarded by the Optical Science and Technology Society for his contribution to the technology of femtosecond laser initiated nanofabrication in 2002. He was a recipient of the Outstanding Young Scientist Award by the Ministry of Education, Culture, Ports, Science and Technology, Japan, in 2006.